AJNR

Sandlike Appearance of Virchow-Robin Spaces in Early Multiple Sclerosis: A Novel Neuroradiologic Marker

Anat Achiron and Meir Faibel

AJNR Am J Neuroradiol 2002, 23 (3) 376-380
http://www.ajnr.org/content/23/3/376

AJNR Am J Neuroradiol 23:376–380, March 2002

Sandlike Appearance of Virchow-Robin Spaces in Early Multiple Sclerosis: A Novel Neuroradiologic Marker

Anat Achiron and Meir Faibel

BACKGROUND AND PURPOSE: **The distinctive hyperintensity of multiple sclerosis (MS) lesions on T2-weighted brain MR images is well recognized. However, Virchow-Robin spaces (VRSs), especially in early MS, have not been described. Our purpose was to determine the frequency of VRSs in recent-onset MS.**

METHODS: **Brain MR imaging was performed in 71 patients (mean age, 26.8 years; range, 20–41 years; 47 women, 24 men) within 3 months of MS onset. Proton density–, T2-, and T1-weighted images were obtained. Age-and sex-matched control subjects (mean age, 27.2 years; range, 22–41 years; 38 women, 22 men) who underwent brain MR imaging as a part of headache evaluation, and findings that were interpreted as normal served as controls. On high-convexity images (axial sections above the upper corpus callosum border), VRSs were identified as small (<2-mm diameter) sandlike areas isointense to CSF. VRSs were graded 0–3.**

RESULTS: **VRSs were visualized in high-convexity white matter in 55% of patients and 7% of control subjects ($P < .001$). In patients, 15% of VRSs were grade 1 (fewer than four), 23% were grade 2 (four to seven), and 62% were grade 3 (more than seven). In control subjects, all identified VRSs were grade 1. Among patients with and those without VRSs, age at onset, neurologic disability, and specific functional system involvement or mono- versus polysymptomatic involvement at onset did not differ.**

CONCLUSION: **VRSs were more frequent in patients with recent-onset MS than in control subjects. The sandlike appearance of VRSs may be a neuroradiologic marker that reflects early inflammatory changes in MS.**

Virchow-Robin spaces (VRSs) are pia-lined extensions of the subarachnoid space around perforating arteries and emerging veins as they penetrate the brain parenchyma and enter or leave the brain on its surface (1). Deeper in the brain, the VRSs are lined by the basement membrane of the glia limitans peripherally, while the outer surfaces of the blood vessels lie centrally. These pial layers form the VRSs as enclosed spaces filled with fluid that is separated from the CSF by the pia of the subarachnoid space (2).

VRSs frequently are detected as small foci with signal intensity equal to that of CSF at brain MR imaging with all pulse sequences. They are present in the anterior perforated substance—around the anterior commissure at the level of the inferior third of the basal ganglia—on both sides. Infrequently, VRSs are seen in the high-convexity white matter extending into the centrum semiovale and follow the route of penetrating cortical arterioles (3, 4). The artery itself, contained within the VRSs, is not identifiable on MR images because it is smaller than 0.4 mm, which is beyond the resolution of the machine and because the associated perivascular space is much larger.

That VRSs smaller than 2 mm in diameter are found in patients of all ages and that they probably represent normal anatomy has been reported. Heier et al (4) reported that they appear in 23% of healthy subjects younger than 20 years, in 33% of those aged 21–40 years, in 28% of those aged 41–60 years, in 33% of those aged 60–80 years, and in 18% of those older than 80 years. High-convexity spaces are less common and appear in only 13% of the healthy population, compared with lenticulostriate VRSs, which occur in 35% of examined subjects. In healthy persons aged 21–40 years, high-convexity VRSs were reported to occur only in 7% (4). The most common causes associated with enlarged VRSs (>2 mm in diameter) were age, hypertension, dementia, and incidental white matter lesions (4, 5).

Received April 17, 2001; accepted after revision August 17.

From the Multiple Sclerosis Center (A.A.) and Neuroradiology Unit (M.F.), Sheba Medical Center, Tel-Hashomer, Israel.

Address reprint requests to Anat Achiron, MD, PhD, Multiple Sclerosis Center, Sheba Medical Center, Tel-Hashomer, 52621, Israel.

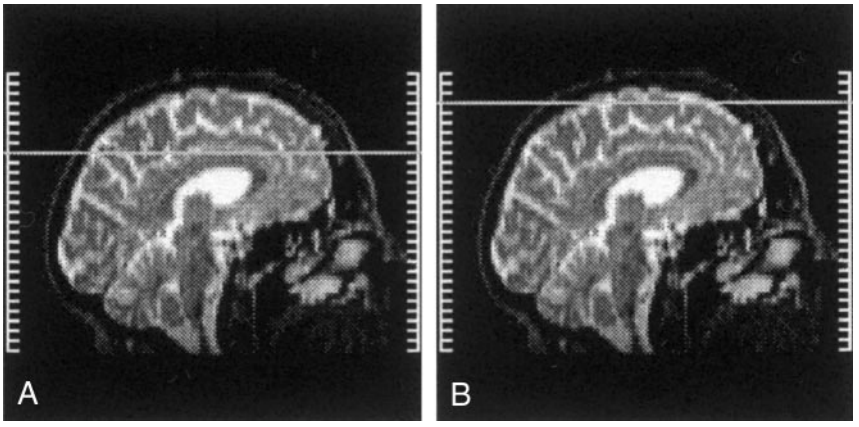

FIG 1. Midsagittal brain sections depict the anatomic level of the high-convexity images. VRSs were identified within these images.
A, Upper border of the corpus callosum.
B, Upper level of the brain.

On MR images, the lesions of multiple sclerosis (MS) are hyperintense relative to brain parenchyma on long-TR images (both short and long TEs) and hypointense on T1-weighted images. VRSs are isointense relative to CSF on images obtained with all pulse sequences.

We have observed multiple high-convexity VRSs, which simulate a sandlike appearance, on brain MR images in several patients during the first episode of neurologic symptoms suggestive of MS. In the present study, we systematically evaluated the incidence of VRSs and the possible correlation between their presence in early MS with various clinical disease parameters. The aim was to improve our understanding of MS pathogenesis and facilitate MR imaging–based classification of VRSs that reflects the distinct disease stages and prognosis.

Methods

Patients and Subjects

We retrospectively assessed MR images in 71 consecutive patients (mean age, 26.8 ± 9.2 years, range, 20–41 years; 47 women, 24 men) within 3 months of the first onset of neurologic symptoms suggestive of MS. At the time of MR imaging, all patients had a diagnosis of probable MS according to the Poser criteria (6), and they had positive brain MR images according to Fazekas criteria (at least four focal lesions involving the white matter or three lesions if one was periventricular in location) (7). A patient's data were included in the final analysis only if the diagnosis of definite MS was confirmed later. All patients underwent thorough neurologic examinations and follow-up for at least 1 year.

Sixty age- and sex-matched control subjects (mean age, 27.2 ± 8.4 years; range, 22–41 years; 38 women, 22 men) with headaches underwent neurologic examination and brain MR imaging as a part of the evaluation of their headaches, and they had no abnormal findings with both. MR imaging was performed in the control subjects with the same MR imaging protocol used in the patients with MS. Images were evaluated for the presence of VRSs, and the VRSs were graded.

MR Imaging

Brain MR imaging was performed with a 2.0-T magnet (Elscint; Haifa, Israel). Imaging sequences consisted of the following: 1) T1-weighted spin-echo sequence in the sagittal and axial planes (550/12 [TR/TE]) performed before and after the injection of gadolinium-based contrast material and 2) a long TR–dual-TE sequence in the axial and coronal planes (5 500/16, 128/1; 256 × 256 matrix; 24 × 24-cm field of view). The MR images covered the brain from the level of the foramen magnum to the high convexity of the scalp, and each examination resulted in the acquisition of 44 sections (3-mm section thickness, no gap) with each technique. Measurements were obtained on long-TR images (T2 weighted) of the high-convexity brain regions; these were defined as all axial sections above the upper border of the corpus callosum, depicted on the mid sagittal brain section (Fig 1). Contrast agent enhancement was used to exclude small enhancing lesions related to MS.

Definition of VRSs

VRSs were identified according to the following criteria: 1) punctuate areas that were isointense to the CSF on images obtained with all pulse sequences, 2) areas that were smaller than 2 mm in diameter, 3) areas conforming to the path of penetrating arteries, and 4) areas that had no mass effect (4, 8). The appearance of the VRSs was recorded only on high-convexity section s that did not include the lenticulostriate area. MS lesions were identified as areas that were hyperintense relative to the brain parenchyma on both long-TR images (short and long TEs) and hypointense on T1-weighted images. They were excluded from the quantification.

Quantification of VRSs

To obtain maximal differentiation between VRSs and small MS lesions, which could also be isointense relative to CSF, only VRSs with a diameter smaller than 2 mm were included in the quantification. Two raters (A.A., M.F.) used a modification of the scale developed by Heier et al (4), which was as follows: grade 0, no VRSs identified; grade 1, fewer than four VRSs identified; grade 2, four to seven VRSs identified; and grade 3, more than seven VRSs identified.

Statistical Analysis

Data are presented as the mean ± the SD. The Fisher exact test was used to compare the groups. The Spearman correlation test was used to analyze the correlation between the presence of VRSs and various clinical parameters. All tests were two tailed, and a P value of .05 or less was considered to indicate a statistically significant difference. For the calculation of the interrater agreement index, we used the following equation (9, 10): $[1 - (Xa - Xb)] \div [(Xa + Xb)/2]$, where Xa and Xb are the measurements obtained by two raters in evaluating images from the same examination. The data were analyzed by using the SAS statistical software package.

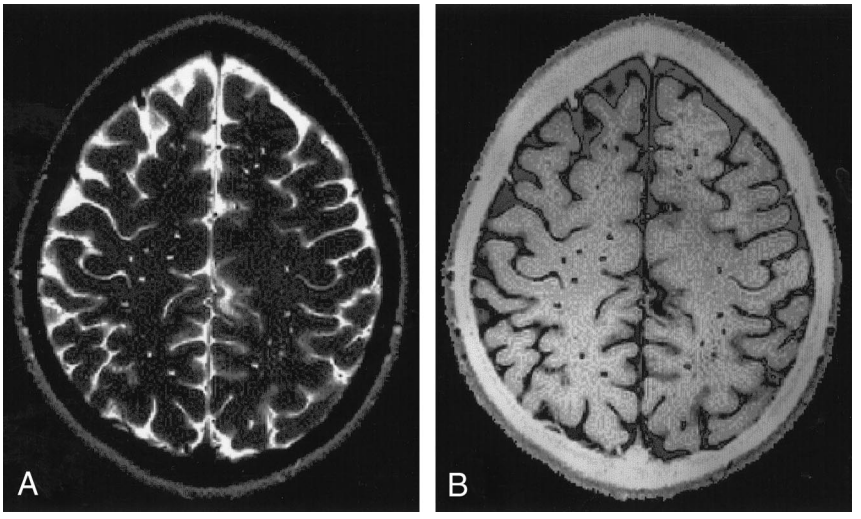

FIG 2. Axial high-convexity MR images show grade 3 VRSs with a sandlike appearance.
A, T2-weighted image (5500/128).
B, T1-weighted image (550/12).

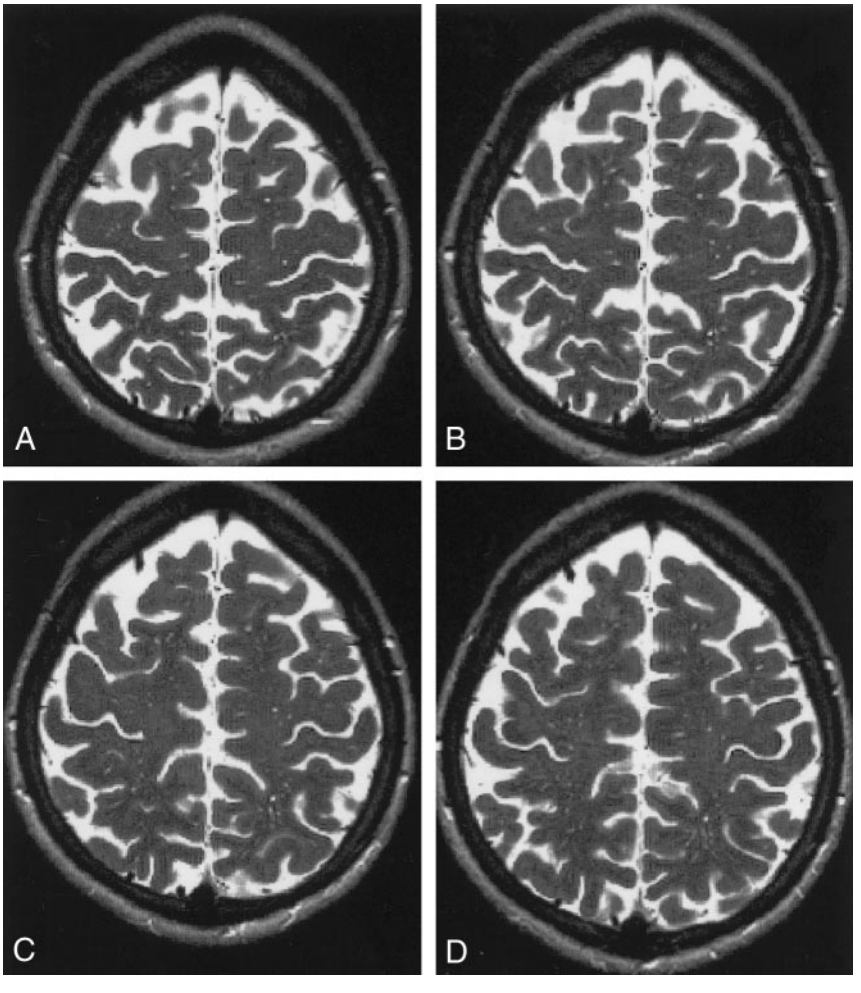

FIG 3. Consecutive axial high-convexity T2-weighted MR images (5500/128) show VRSs. Image in *A* is most superior; image in *D*, most inferior.

Results

The VRSs resembled small isointense sandlike grains within the white matter on T1- and T2-weighted images (Fig 2). The appearance of VRSs in consecutive high-convexity T2-weighted images is demonstrated in Figure 3.

VRSs were visualized in 39 (55%) of 71 patients with probable MS and in four (7%) of 60 control subjects. This difference was statistically significant ($P < .001$). Interrater agreement for VRSs estimates was 98% for grade 1 assessments, 96% for grade 2 assessments, and 98% for grade 3 assessments.

The distribution of VRSs in the group with MS (n = 39) was as follows: grade 1, six (15%); grade 2,

nine (23%); and grade 3, 24 (62%). In control subjects, all high-convexity VRSs were grade 1. Among patients with MS, no differences were found between patients with and those without identified VRSs in relation to age of onset, neurologic disability, specific functional system involvement, and monoversus polysymptomatic involvement at onset. These findings suggested that patients with VRSs (55%) did not differ in these clinical parameters from patients without identified VRSs (45%).

In patients with MS no correlations were found between the grade of VRSs and age of onset, neurologic disability, specific functional system involvement, mono- or polysymptomatic involvement, or number of contrast-enhancing lesions at onset.

Discussion

We evaluated the frequency and grade of VRSs demonstrated on MR images obtained in the white matter of the high cerebral convexity during the onset of MS. VRSs were identified in 55% of patients with MS during the onset of the disease and in only 7% of age- and sex-matched healthy subjects. To our knowledge, this is the first report in the literature involving the study VRSs in a population with MS. Specifically, grade 3 (more than seven) VRSs were present in 34% of patients with MS during disease onset, and they were not present in the control subjects. The increased number of small (<2-mm-diameter) VRSs, which had a sandlike appearance within the high convexity of the brain, did not correlate with any of the clinical or demographic disease parameters at disease onset. This lack of correlation is not surprising, becuase most MR imaging parameters are not correlated with clinical parameters at disease onset. An evaluation of whether the presence of VRSs at onset has prognostic implications on the future development of MS is important.

VRSs are considered to be immunologic spaces in which macrophages bearing major histocompatability complex class II antigens can trap foreign antigens entering the brain and either process them locally to lymphocytes or convey them to local lymph nodes (11, 12). Thus, the role of the VRSs is associated with the transport of soluble factors between the extracellular fluid of the brain and the CSF, as was demonstrated with ultrastructural studies and intracerebrally injected tracer substances (13). Consequently, a full-blown immune response can be generated within the VRSs once large numbers of activated macrophages and T and B lymphocytes accumulate locally. Findings of immunocytochemical studies confirm the presence of mononuclear perivascular phagocytic cells in the VRSs; it was shown in animal experiments that cervical drainage blockade resulted in the distension of VRSs caused by protein-rich fluid (14). In addition, immunologic reactions can occur within the VRSs by perivascular macrophages and endocytosis (11), and endogenous serum proteins (immunoglobulin G, complement C9, immunoglobulin M) were identified in the VRSs (15). These findings have important clinical implications regarding experimental and pathologic autoimmune dysfunction within the brain, because they suggest that blood-borne macromolecular components of the immune cascade gain passive widespread entry to the CNS parenchyma and perivascular spaces. This passive entry could provide an access for potential autoimmune antibodies and autoreactive T cells to initiate an immune response against CNS peptides. Also, it can explain the occurrence of an inflammatory process within the brain, even in the absence of overt blood-brain barrier derangement or disruption.

In MS, the typical demyelinating lesions are characteristically situated around veins or on pial or ependymal surfaces. Cuffs of inflammatory cells in VRSs are prominent features of acute MS plaques (16). This perivascular accumulation of cells may simply reflect an overflow of the immune response, or it raises the possibility that the stimulating antigen is confined to cells in the periventricular space. The continuous exposure of VRSs perivascular phagocytes to blood-borne potential antigens may be the route through which an autoimmune cascade is triggered. The leakiness of vessels in the subarachnoid space during the inflammatory process of demyelination suggests increased permeability and widespread, rapid entry of inflammatory cells from the blood to the CNS. This process can account for the high levels of immunoglobulin G within the CSF in patients with MS (17, 18) and explain the involvement of complement activation in mediating oligodendrocyte damage (19).

In the animal model of MS with both acute and chronic experimental autoimmune encephalomyelitis, the initial pathologic finding detected was an increased number of inflammatory cells in the subarachnoid space; this finding was followed by the detection of the cells in the VRSs before the animals had any neurologic impairment. These stages preceded perivascular infiltration of inflammatory cells in the parenchyma (12, 20).

In other inflammatory diseases involving the white matter, such as canine globoid cell leukodystrophy and sarcoidosis, inflammatory infiltrates consisting of macrophages and lymphocytes were present within the VRSs (21–23). In CNS cryptococcosis in patients with AIDS, enlarged VRSs were present as an earlier manifestation at brain MR imaging (24), and immunocytochemical stains demonstrated clusters of macrophages containing cryptococci within the VRSs (25). Similarly, in early lacunar infarcts and in mucopolysaccharidosis, fatty macrophages were present in enlarged VRSs (26, 27), whereas in diffuse carcinomatous leptomeningeal metastases, extensive involvement of the subarachnoid space with tumor cells was associated with dense neoplastic infiltration of the VRSs (28). The findings of all these studies support the important role of VRSs as important immunologic sites in which macrophages react to foreign antigens (11).

Conclusion

We suggest that the increased number of VRSs, which resemble sandlike grains on high-convexity brain MR images, is the result of the local brain inflammation that is characteristic of MS. During the early phase of the disease, inflammatory cells that contribute to the active process of demyelination penetrate the VRSs. Their appearance could serve as an additional neuroradiologic marker in the diagnosis of the disease.

References

1. Hutchings M, Weller RO. **Anatomical relationships of the pia mater to cerebral blood vessels in man.** *J Neurosurg* 1986;65:316–325
2. Zhang ET, Inman CB, Weller RO. **Interrelationships of the pia mater and the perivascular (Virchow-Robin) spaces in the human cerebrum.** *J Anat* 1990;170:111–123
3. Jungreis CA, Kanal E, Hirsch WL, et al. **Normal perivascular spaces mimicking lacunar infarction: MR imaging.** *Radiology* 1988; 169:101–104
4. Heier LA, Bauer CJ, Schwartz L, Zimmerman RD, Morgello S, Deck MD. **Large Virchow-Robin spaces: MR-clinical correlation.** *AJNR Am J Neuroradiol* 1989;10:929–936
5. Bokura H, Kobayashi S, Yamaguchi S. **Distinguishing silent lacunar infarction from enlarged Virchow-Robin spaces: a magnetic resonance imaging and pathological study.** *J Neurol* 1998;245:116–122
6. Poser CM, Paty DW, Scheinberg L, et al. **New diagnostic criteria for multiple sclerosis: guidelines for research protocols.** *Ann Neurol* 1983;13:227–231
7. Fazekas F, Barkhof F, Filippi M, et al. **The contribution of magnetic resonance imaging to the diagnosis of multiple sclerosis.** *Neurology* 1999;53:448–456
8. Braffman BH, Zimmerman RA, Trojanowski JQ, Gonatas NK, Hickey WF, Schlaepfer WW. **Brain MR: pathologic correlation with gross and histopathology, I: lacunar infarction and Virchow-Robin spaces.** *AJR Am J Roentgenol* 1988;151:551–558
9. Filippi M, Horsfield MA, Bressi S, et al. **Intra- and inter-observer agreement of brain MRI lesion volume measurements in multiple sclerosis: a comparison of techniques.** *Brain* 1995;118:1593–1600
10. Bland JM, Altman DG. **Statistical methods for assessing agreement between two methods of clinical measurement.** *Lancet* 1986; 1:307–310
11. Esiri MM, Gay D. **Immunological and neuropathological significance of the Virchow-Robin space.** *J Neurol Sci* 1990;100:3–8
12. Matsumoto Y, Fujiwara M. **The immunopathology of adoptively transferred experimental allergic encephalomyelitis (EAE) in Lewis rats, I: immunohistochemical examination of developing lesions of EAE.** *J Neurol Sci* 1987;77:35–47
13. Becker NH, Novikoff AB, Zimmerman HM. **Fine structure observations of the uptake of intravenously injected peroxidase by the rat choroid plexus.** *J Histochem Cytochem* 1967;15:160–165
14. Foldi M. **Prelymphatic-lymphatic drainage of the brain.** *Am Heart J* 1977;93:121–124
15. Broadwell RD, Sofroniew MV. **Serum proteins bypass the blood-brain fluid barriers for extracellular entry to the central nervous system.** *Exp Neurol* 1993;120:245–263
16. Prineas J. **Pathology of the early lesion in multiple sclerosis.** *Hum Pathol* 1975;6:531–554
17. Tourtellotte WW, Ma BI. **Multiple sclerosis: the blood-brain-barrier and the measurement of de novo central nervous system IgG synthesis.** *Neurology* 1978;28:76–83
18. Compston A, Scolding N, Wren D, Noble M. **The pathogenesis of demyelinating disease: insights from cell biology.** *Trends Neurosci* 1991;14:175–182
19. Scolding NJ, Morgan BP, Houston WA, Linington C, Campbell AK, Compston DA. **Vesicular removal by oligodendrocytes of membrane attack complexes formed by activated complement.** *Nature* 1989;339:620–622
20. Raine CS, Snyder DH, Valsamis MP, Stone SH. **Chronic experimental allergic encephalomyelitis in inbred guinea pigs: an ultrastructural study.** *Lab Invest* 1974;31:369–380
21. Yajima K, Fletcher TF, Suzuki K. **Canine globoid cell leukodystrophy, I: further ultrastructural study of the typical lesion.** *J Neurol Sci* 1977;33:179–197
22. Moore GR, Raine CS. **Leptomeningeal and adventitial gliosis as a consequence of chronic inflammation.** *Neuropathol Appl Neurobiol* 1986;12:371–378
23. Mirfakhraee M, Crofford MJ, Guinto FC, Nauta HJ, Weedn VW. **Virchow-Robin space: a path of spread in neurosarcoidosis.** *Radiology* 1986;158:715–720
24. Miszkiel KA, Hall-Craggs MA, Miller RF, Kendall BE, Wilkinson ID, Paley MN, Harrison MJ. **The spectrum of MRI findings in CNS cryptococcosis in AIDS.** *Clin Radiol* 1996;51:842–850
25. Lee SC, Dickson DW, Casadevall A. **Pathology of cryptococcal meningoencephalitis: analysis of 27 patients with pathogenetic implications.** *Hum Pathol* 1996;27:839–847
26. Fisher CM. **Lacunar strokes and infarcts: a review.** *Neurology* 1982;32:871–876
27. Murata R, Nakajima S, Tanaka A, et al. **MR imaging of the brain in patients with mucopolysaccharidosis.** *AJNR Am J Neuroradiol* 1989;10:1165–1170
28. Klein P, Haley EC, Wooten GF, VandenBerg SR. **Focal cerebral infarctions associated with perivascular tumor infiltrates in carcinomatous leptomeningeal metastases.** *Arch Neurol* 1989;46:1149–1152